NeuroImage 83 (2013) 658–668

Contents lists available at ScienceDirect

NeuroImage

journal homepage: www.elsevier.com/locate/ynimg

Structural brain correlates of human sleep oscillations

Jared M. Saletin [a], Els van der Helm [a], Matthew P. Walker [a,b,*]

[a] Sleep and Neuroimaging Laboratory Department of Psychology, University of California, Berkeley, CA 94720-1650, USA
[b] Helen Wills Neuroscience Institute, University of California, Berkeley, CA 94720-1650, USA

ARTICLE INFO

Article history:
Accepted 4 June 2013
Available online 14 June 2013

Keywords:
Sleep spindles
Slow waves
Gray matter
VBM
EEG
NREM sleep

ABSTRACT

Sleep is strongly conserved within species, yet marked and perplexing inter-individual differences in sleep physiology are observed. Combining EEG sleep recordings and high-resolution structural brain imaging, here we demonstrate that the morphology of the human brain offers one explanatory factor of such inter-individual variability. Gray matter volume in interoceptive and exteroceptive cortices correlated with the expression of slower NREM sleep spindle frequencies, supporting their proposed role in sleep protection against conscious perception. Conversely, and consistent with an involvement in declarative memory processing, gray matter volume in bilateral hippocampus was associated with faster NREM sleep spindle frequencies. In contrast to spindles, gray matter volume in the homeostatic sleep-regulating center of the basal forebrain/hypothalamus, together with the medial prefrontal cortex, accounted for individual differences in NREM slow wave oscillations. Together, such findings indicate that the qualitative and quantitative expression of human sleep physiology is significantly related to anatomically specific differences in macroscopic brain structure.

Introduction

Sleep is strongly conserved across phylogeny. In humans, sleep EEG physiology is remarkably stable within an individual from one night to the next (Werth et al., 1997). However striking differences in these same sleep EEG features are observed from one individual to the next (De Gennaro et al., 2005), the reasons for which are largely unknown. Most prominent are inter-individual differences in non-rapid eye movement (NREM) sleep, specifically slow waves (Mongrain et al., 2006; Tucker et al., 2007; Viola et al., 2012) and sleep spindles (De Gennaro et al., 2005; Werth et al., 1997). Furthermore, these sleep EEG features demonstrate evidence of partial genetic determination (Vandewalle et al., 2009; Viola et al., 2007), further suggesting that they represent a stable, trait-like physiological property. Here, we examine one potential factor explaining these trait inter-individual differences in sleep EEG physiology—brain structure. The morphology of the brain is a known determinant of function, evidenced by circumstances of development, degeneration, and brain damage (Kanai and Rees, 2011). Despite such relationships, the possibility that individual differences in human brain structure predict individual differences in sleep physiology remains largely uncharacterized.

Candidate anatomical regions of interest that may explain individual differences in sleep spindles and slow waves emerge both from their identified electrical source generators and the proposed functions they support. For example, sleep spindles have been implicated in the inhibitory "gating" of exteroceptive and interoceptive sensory perception (De Gennaro et al., 2005), thereby preserving the sleep state from both exogenous (e.g. audition (Dang-Vu et al., 2010a)) and endogenous (e.g. pain (Landis et al., 2004)) sources. This protective function appears to be dependent upon mutually inhibitory thalamo-cortical circuitry (Contreras and Steriade, 1996; De Gennaro and Ferrara, 2003), implicating the thalamus as one potential structural region of interest (ROI) accounting for inter-individual differences in trait-varying properties of sleep spindles. Additional candidate ROIs are represented by downstream auditory cortex and insular cortex, where the processing of potentially sleep-disrupting exogenous and endogenous stimuli occur. Indeed, functional neuroimaging reports have described activation in both primary auditory (Dang-Vu et al., 2008a) and insula cortices (Schabus et al., 2007) during the occurrence of sleep spindle events. Finally, and contrasting with a sleep-protective role, an emerging function assigned to faster frequency spindles has focused on hippocampal-dependent memory processing (Diekelmann and Born, 2010). Inter-individual differences in faster frequency sleep spindles predict hippocampal-dependent learning ability (Mander et al., 2011). Furthermore, faster frequency sleep spindle events coincide with hippocampal activation, as assessed by event-related fMRI (Schabus et al., 2007).

As with spindles, target anatomical regions that may contribute to inter-individual difference in slow wave features are informed by reports examining the functional properties of slow waves (including density and amplitude). The basal forebrain represents one such

* Corresponding author at: Department of Psychology, Tolman Hall 3331, University of California, Berkeley, CA 94720-1650, USA. Fax: +1 510 642 5293.
E-mail address: mpwalker@berkeley.edu (M.P. Walker).

1053-8119/$ – see front matter © 2013 Elsevier Inc. All rights reserved.
http://dx.doi.org/10.1016/j.neuroimage.2013.06.021

candidate due to its well defined role in sleep homeostasis and regulation (Modirrousta et al., 2007), governing changes in slow wave density following prolonged wakefulness (Mistlberger et al., 1987). Beyond the basal forebrain, midline prefrontal cortex and insula cortex both represent additional target regions of interest accounting for slow wave differences between individuals, particularly their amplitude. For example, slow waves are not simply dominant over topographic midline prefrontal EEG derivations (Feinberg et al., 2011), but these frontal derivations also display the greatest extent of inter-individual variability in slow waves as a function of genotype (Viola et al., 2012) and chronotype (Mongrain et al., 2006). Moreover, inter-individual differences in the homeostatic rebound of slow waves following sleep deprivation are similarly observed in the EEG over midline prefrontal cortex (Goel et al., 2009; Rusterholz and Achermann, 2011). EEG source analyses of slow waves have localized source generators not only in the cingulate cortex, consistent with a midline prefrontal dominance of slow waves, but also in the insula cortex (Murphy et al., 2009). The known cytoarchitecture of the insula cortex and its connectivity to the prefrontal cortex have therefore been proposed to support propagation of slow waves between these potential generator regions (Petrides and Pandya, 1999; van der Kooy et al., 1982).

Guided a priori by these candidate regions, here, we examine whether macroscopic differences in human brain structure, indexed by gray matter volume, explain stable inter-individual variability (De Gennaro et al., 2005) in the canonical oscillations of sleep: sleep spindles and slow waves.

Materials and methods

Twenty-two healthy adults (21.2 ± 2.25 years [mean ± s.d.], (range 19–26), 10 males) participated in the study. Exclusion criteria, assessed using a pre-screening questionnaire, included a history of sleep disorders, neurologic disorders or closed head injury, Axis I psychiatric disorders according to the DSM-IV criteria encompassing major mental disorders, history of drug abuse, and current use of anti-depressant or hypnotic medication. The participants abstained from alcohol and caffeine for a minimum of 48 h prior to sleep recording. Additionally, sleep schedules were standardized prior to in-lab recordings (7–9 h of sleep per night, with morning wake time between 06:30 and 08:30), as verified by nightly sleep logs. The study was approved by the local human studies committee, with all the participants providing their written informed consent.

Polysomnography recording and sleep stage classification

Polysomnography (PSG) sleep monitoring was recorded using a Grass Technologies Comet XL system (Astro-Med, Inc., West Warwick, RI). Electroencephalography (EEG) was recorded at 19 standard locations conforming to the International 10-20 System (Jasper, 1958) (FP1, FP2, F7, F3, FZ, F4, F8, T3, C3, CZ, C4, T4, T5, P3, PZ, P4, T6, O1, O2). Electrooculography (EOG) was recorded at the right and left outer canthi (right superior; left inferior). Electromyography (EMG) was recorded via three electrodes (one mental, two sub-mental). Finally, electrocardiography (ECG) was recorded using two electrodes: below the left and the right clavicle. Reference electrodes were placed at both the left mastoid and the right mastoid (A1, A2). Data were digitized at 400 Hz. All data were stored unfiltered (recovered frequency range of 0.1–100 Hz), except for a 60 Hz notch filter. For recording only, each channel was referenced to a forehead scalp reference. Sleep staging was performed in accordance with standardized techniques (Rechtschaffen and Kales, 1968) from the C3–A2 derivation, and NREM–REM cycles were defined according to modified criteria of Feinberg and Floyd, 1979 (Aeschbach and Borbély, 1993).

Polysomnography EEG signal processing

Following sleep scoring, each EEG channel was re-referenced to the average of the left and right mastoids for quantitative signal processing. All EEG analyses were performed in MATLAB 7.5 (The Mathworks, Natick, MA), including the add-in toolbox EEGLAB (http://sccn.ucsd.edu/eeglab/). The EEG was band-passed filtered offline (EEGLAB function eegfilt) using Finite Impulse Response (FIR) filters (low-pass at 50 Hz, high-pass at 0.5 Hz). A high-pass cut-off frequency of 0.5 Hz was chosen to remove possible slow artifact in the EEG. Signals were then visually marked for artifact in 5-second epochs. These 5-second epochs, used for artifact-rejection, were then sorted by sleep stages for analysis.

Slow waves were detected using an established procedure (Kurth et al., 2010; Massimini et al., 2007; Murphy et al., 2009; Riedner et al., 2007). Following artifact rejection, a low-pass FIR filter was applied to EEG data removing all activity above 4 Hz (yielding a frequency distribution of (0.5–4 Hz, as in previous slow wave detection analyses) (Kurth et al., 2010; Massimini et al., 2007; Murphy et al., 2009; Riedner et al., 2007). In short (but see (Riedner et al., 2007) for details) the algorithm determines negative and positive peaks occurring in the EEG time series after each zero-crossing (change in amplitude from negative-to-positive, or vice-versa), detecting slow waves in each channel independently. Multiple peaks occurring between zero-crossings were considered part of the same slow wave. Waves were then sorted according to sleep stage. Any detections occurring during Stage 1 were excluded from analysis. Further, analyses were limited only to defined NREM periods (Aeschbach and Borbély, 1993). Finally, all waves occurring within artifact-marked 5-second epochs were removed from analysis. Analysis of slow waves slow waves focused on two orthogonal metrics — amplitude and density, respectively (slow wave activity (SWA; power in the 0.75–4.75 Hz band) was not chosen since this composite measure cannot distinguish between the amplitude of slow waves and their rate of incidence (density) (Carrier et al., 2011). For slow wave amplitude, the negative peak (μV) of each NREM slow wave was averaged to create a single NREM average for each EEG channel, in each subject. Slow wave density was calculated as the number of artifact-free detected slow waves in each channel divided by the amount of artifact-free NREM sleep time recorded, resulting in a single NREM value for each EEG channel, in each subject. Both slow wave metrics were then included in the MRI regression analyses, with parameters derived from the Fz (frontal midline) EEG derivation chosen, due to the known topography and concentration of slow waves over midline frontal cortex, both in the current study (Fig. 4), and prior reports (Dang-Vu et al., 2008b; Kurth et al., 2010; Murphy et al., 2009; Riedner et al., 2007).

Sleep spindles were detected for each channel of EEG by an established automatic algorithm (Ferrarelli et al., 2007; Mander et al., 2011; Saletin et al., 2011). Band-pass FIR filters were first applied to EEG sleep data (spindle range: high-pass: 11 Hz; low-pass: 15 Hz), restricting only those events falling within the spindle frequency range (11–15 Hz) (Schabus et al., 2007). Examining the broad spindle band (11–15 Hz) rather than limiting analyses to previously defined slow (11–13 Hz) or fast (13–15 Hz) bands allows unbiased determination of individual spindle frequency known to vary broadly, in trait-like manner across individuals (Werth et al., 1997). NREM epochs were then extracted (NREM stages 2, 3 and 4) based on visual scoring and all artifact-free epochs were then concatenated into one continuous NREM time series for analysis. The amplitude of the rectified signal from NREM sleep was used as a unique time series, identifying amplitude fluctuations exceeding channel-wise threshold values, with the lower and upper values set at two and eight times the average amplitude for each channel separately. The boundaries of spindle events were then defined when amplitude fluctuations dropped below the cutoff threshold. For each participant, spindle frequency was calculated for each spindle defined as the number of peaks

in the EEG signal occurring within the spindle event, divided by the duration of the spindle, yielding a frequency measure in cycles per second (Hz). Channel-specific NREM average spindle frequency was determined by then averaging across the frequencies of all detected spindles in each channel. Individual-wise spindle frequency across the broad range of spindle frequencies, unlike other parameters such as amplitude or density, demonstrates stable trait-like inter-individual differences, previously described as a purported sleep spindle "fingerprint" within individuals, stable across multiple nights (De Gennaro et al., 2005; Werth et al., 1997). Sleep spindles have a known topography as a function of frequency. Slow spindles are frontal dominant, while fast spindles show parietal dominance (De Gennaro and Ferrara, 2003; Mander et al., 2011; Saletin et al., 2011; Schabus et al., 2007). To most fully describe inter-individual variability in spindle frequency we examined spindles across the entire (11–15 Hz) frequency range. In an attempt to remove the influence of this topography on subject-wise metrics of spindle frequency, frequency estimates (itself an average of individual events) were averaged over traditional midline electrodes (frontal (Fz), central (Cz) and parietal (Pz), rather than using any one single electrode for analysis. This average allowed for the characterization of an individual's average spindle frequency across the anterior/posterior head axis, allowing for equal contribution of slow- and fast-spindle frequency across these spindle-dominant areas. Following averaging, each individual's representative spindle frequency was used in structural imaging regression analyses.

EEG source localization of slow waves

EEG source analysis of slow waves (Murphy et al., 2009) was additionally performed to allow assessment of whether potential structural brain correlates of NREM slow waves converged on homologous regions associated with the electrical generation of slow waves. Standardized low resolution brain electromagnetic tomography (sLORETA) (Pascual-Marqui, 2002) was calculated for the EEG at the negative peak of the slow wave, as described below. No source analysis was performed for sleep spindles, as, unlike slow waves, the spindle is a multi-peak oscillation. While studies have attempted to source components of sleep spindle activity (Ventouras et al., 2007), or to discrete frequency bins across a band (Anderer et al., 2001), there is no clear spindle-analogue sLORETA calculation for spindles as with the slow wave. Therefore, only sLORETA of slow waves was performed. The sLORETA approach to source analysis computes solutions using a head model based on the MNI152 template (Mazziotta et al., 2001). Solution space is limited to cortical gray matter, making sLORETA more precise than other methods of source localization that are not anatomically constrained, and is made up of 6239 voxels at 5 mm resolution (Pascual-Marqui, 2002). While the anatomical precision of sLORETA, and of all source analysis techniques, varies depending on the number of electrodes in the EEG montage (Laarne et al., 2000), numerous studies have employed source analysis using montage arrays of similar or lower resolution to the current study, indicating sufficient coverage of the scalp to provide robust source estimates (Bela et al., 2007; Clemens et al., 2008; Clemens et al., 2009; Isotani et al., 2001; Pascual-Marqui et al., 1999; Ponomarev et al., 2010; Tislerova et al., 2008; Veiga et al., 2003). Interpretation of sLORETA findings is limited to the lobular level of resolution, and not beyond, fitting with prior expectations of this array density (Bela et al., 2007; Clemens et al., 2008, 2009; Isotani et al., 2001; Pascual-Marqui et al., 1999; Ponomarev et al., 2010; Tislerova et al., 2008; Veiga et al., 2003). Consistent with previous EEG source analyses of slow waves (Murphy et al., 2009), NREM filtered (0.5–4 Hz) was marked at the maximal negative peak of each slow wave (detected at Fz, based on wave amplitude topography). In an event-related potential approach, 1-second epochs were extracted around the negative peak (500 ms on either side). Each epoch, corresponding to one wave, was averaged within-subject and then between-subjects, yielding a single grand average epoch for the group (each individual participant's FZ average epoch depicted in Fig. 4). Finally, this 1-second epoch was submitted to sLORETA analyses in the time-domain. Source localization was centered on the negative peak of the grand-average waveform.

Structural magnetic resonance imaging

Structural MRI was performed on a Siemens Magnetom Trio 3T scanner equipped with a 32-channel head coil. Two concomitant high-resolution MPRAGE T1-weighted anatomical scans were obtained for each participant, each consisting of 176 sagittal slices (1 mm isotropic voxels) acquired with a repetition-time (TR) of 2300 ms and an echo-time (TE) of 2.52 ms. Individual estimates of gray matter volume, a stable trait-like measure previously demonstrated to offer sensitivity to inter-individual variability in brain morphology (Thompson et al., 2001), was calculated using the validated voxel-based morphometry approach (VBM) (Ashburner and Friston, 2000; Dumontheil et al., 2010; Mak et al., 2011; Ridgway et al., 2009). VBM analysis quantified the signal intensity of each voxel in the brain for a gray matter segmentation image, given the differential signal intensity yielded by magnetic resonance properties of gray and white matter, respectively. These gray matter voxel intensities were entered into whole-brain regression analyses, comparing gray matter volume and a given experimental variable, in this case, sleep EEG physiological parameters. While other methods for gray matter imaging exist, allowing for manual (Neylan et al., 2010) or semi-automated segmentation of brain volumes (Schmitz et al., 2011), the VBM procedure has been repeatedly used and validated for whole-brain imaging of voxel-wise gray matter volume (Celle et al., 2010; Dumontheil et al., 2010; Giorgio et al., 2010; Mak et al., 2011; Mueller et al., 2011; Pereira et al., 2010; Ridgway et al., 2009).

Image processing used Statistical Parametric Mapping (http://www.fil.ion.ucl.ac.uk/spm) in conjunction with the VBM 5.1 Toolbox for SPM5 (http://dbm.neuro.uni-jena.de/vbm/). To maximize signal-to-noise, and therefore the ability to detect structural differences between participants, the two anatomical T1-weighted MPRAGE scans were first realigned (SPM8 Realign: 2nd Degree B-Spline Interpolation) to each other and then averaged. One participant contributed only 1 scan, due to technical issues during acquisition. Segmentation of anatomical images into gray matter (GM), white matter (WM) and cerebral spinal fluid (CSF) was estimated for each participant's mean anatomical scan using the VBM5.1 Toolbox, implementing default settings (Koutsouleris et al., 2009), including iterative weighting of a hidden Markov random field (HMRF). While the standard SPM segmentation uses prior information to estimate the tissue classes of each voxel, VBM5.1 uses a Bayesian approach not dependent on tissue priors, which can allow for greater accuracy in tissue segmentation (Koutsouleris et al., 2009). Following segmentation, DARTEL was used in SPM8 (Ashburner, 2007) to generate a study-specific group template average using standard procedures, including 6 iterations of template fitting, and the use linear elastic energy for regularization. Following template registration, this template was normalized to MNI space and the resulting transformation matrix was used to normalize the DARTEL flow fields and individual tissue images of all 22 subjects into standard space (DARTEL routine: "Normalize to MNI Space"). The normalization maintained a voxel size of 1 mm isotropic, included modulation to preserve regional signal intensities, and included a 8 mm Gaussian FWHM smoothing-kernel to reduce signal-to-noise for statistical analyses.

An explicit thresholding mask based on the signal-to-noise of the data was calculated according to prior procedures (Ridgway et al., 2009), optimizing the threshold of the each individual's gray matter image given the distribution of data across the group as a whole, aiming to remove low-signal noise from analyses. Finally, total intracranial volume (TIV) was calculated from each participant's native-space GM, WM, and CSF segmentations calculated from VBM5.1. Total intracranial

volume was calculated from the native-space tissue maps according to the "get_totals" routine for SPM commonly used to calculate global measures of brain volume in structural imaging studies (e.g. (Ansell et al., 2012; Benedetti et al., 2012; Benedetti et al., 2011; D'Agata et al., 2011; Eckert et al., 2008; Wolk et al., 2009), etc.). This measure of total intracranial volume was verified against an independent analysis using the reconstruction scheme in the different software package FreeSurfer (Fischl and Dale, 2000), which derives intracranial volumes from cortical surface reconstruction, with the two methods resulting in remarkably similar estimates (correlations between the values from each method: $r = 0.924$, $p < 0.0001$). Cross-sectional analyses of EEG data raise concerns of differences in skull thickness that, beyond the electrical signal itself, could lead to amplitude differences. However, considering that the variance of EEG amplitude explained by skull thickness across frontal, temporal and parietal regions ranges from $r^2 = 0.01$ to $r^2 = 0.13$ (Hagemann et al., 2008) it would suggest that any such contribution is likely modest.

Statistical analyses

To examine the bidirectional nature of inter-individual difference in sleep spindle frequency, positive and negative contrast maps were generated, reflecting areas where gray matter volume correlated with increasingly faster, or slower spindle frequency, respectively. Slow wave regression models were then created for the average negative amplitude of the slow waves, and the density of slow waves, in NREM sleep, respectively. Separate statistical models for each analysis were created to minimize the impact of co-linearity between sleep spindles and slow waves (Steriade et al., 1993) and between specific properties of slow waves themselves (Carrier et al., 2011). For the slow wave analyses, one subject was removed from the regression (yielding $n = 21$) based on prominent artifact in their recording within the slow wave frequency range (~0.6 Hz). In all statistical models, proportional scaling to TIV (total intracranial volume) was used to account for total brain size, as in previous VBM studies (Bendlin et al., 2008). The current results did not change when age was included as an additional covariate in the model.

Statistical analysis was performed using a two-step approach, as in previous studies (Altena et al., 2010; Gong et al., 2005; Joo et al., 2009, 2010; Kim et al., 2008; O'Donoghue et al., 2005; Yaouhi et al., 2009). First, at the whole-brain level, uncorrected results were identified at a voxel-wise p-value of 0.001 (30 voxel extent threshold), followed next by analysis of clusters within candidate ROIs that survived this initial threshold. These clusters were subsequently submitted to small volume correction (SVC) at the family-wise-error rate of $p < 0.05$, cluster level (Joo et al., 2009; Kim et al., 2008; Nichols and Hayasaka, 2003; Yaouhi et al., 2009). This two-step analysis approach allowed both for a strict test of our hypothesis-driven ROI targets, while still offering an exploratory investigation of associations outside these ROIs (important, considering that the current study represents a first investigation of structural gray matter associations with sleep EEG physiology in the adult brain). Figures were generated by overlaying statistical images on the ch2better.nii.gz template provided in the MRIcron visualization software, in standardized space. Images for display were thresholded at a $p < 0.005$.

Definition of anatomical regions of interest (ROIs)

For slow wave regression models, SVC was performed on a priori anatomical ROIs derived from convergent source EEG analyses (Murphy et al., 2009) and functional neuroimaging studies (Dang-Vu et al., 2008b; Maquet et al., 1997), resulting in ROIs in bilateral cingulate, insula (anterior and posterior) and orbital frontal cortices (defined within the validated wfu_pickatlas SPM toolbox [www.fmri.wfubmc.edu/cms/software]; (Maldjian et al., 2003). These areas are congruent with the both the results of EEG source analyses (Murphy et al., 2009), as well as known topography dominance of slow waves and their inter-individual differences occurring over midline frontal cortex (Carrier et al., 2011; Esser et al., 2007; Feinberg et al., 2011; Huber et al., 2004; Mongrain et al., 2006; Murphy et al., 2009; Rusterholz and Achermann, 2011). Finally, a mask in the region of the basal forebrain and the hypothalamus was created, identified from neurophysiology studies demonstrating it as the seat of sleep–wake regulation (Kalinchuk et al., 2010; Modirrousta et al., 2007; Monti, 2011), a process that is represented by slow waves in the EEG (Achermann and Borbély, 2003; Esser et al., 2007; Riedner et al., 2007; Tononi and Cirelli, 2006), as well as from neuroimaging findings demonstrating associations between the basal forebrain/hypothalamus and slow wave activity (Dang-Vu et al., 2010b; Maquet et al., 1997). The ROI was defined by creating 8 mm diameter sphere drawn around previously published coordinates (MNI voxel coordinates [x, y, z]: [2, 2, −4]) from a functional neuroimaging study of slow wave sleep (Maquet et al., 1997). The choice of a sphere defined functionally, rather than the use of an anatomical ROI was based upon the known heterogeneity of function within the anatomical region of the basal fore-brain/hypothalamus that prevents the anatomical delineation of sleep-related nuclei at the resolution of structural MRI (Maquet et al., 1997; Szymusiak, 1995). All ROIs are considered independent tests based on differential anatomical networks implicated in the generation and regulation of each different physiological oscillation.

For sleep spindles, ROIs were created based on a priori regions of interest, also using the wfu_pickatlas toolbox. First, based on animal neurophysiology (Steriade et al., 1985) and human functional neuroimaging studies (Schabus et al., 2007) indicating the thalamus in spindle generation, bilateral thalamic ROIs were created. Second, sensory ROIs were constructed building on the proposed role of sleep spindles in protecting sleep against external and internal conscious sensation. ROIs focused on the anatomical cortical regions associated with the two sensory percepts most prevalent to sleep disruption: exteroceptive audition (and interoceptive pain somatosensation (Dang-Vu et al., 2010a; Landis et al., 2004; Pivik et al., 1999). ROIs were generated in bilateral primary auditory cortex (Heschl's gyrus) (Dang-Vu et al., 2008a) and bilateral anterior and posterior insula cortices (Schabus et al., 2007), respectively. Finally, ROIs in the hippocampus were constructed based on growing evidence for the role of sleep spindles in episodic memory processing (Diekelmann and Born, 2010), together with of their coinciding relationship with hippocampus sharp-wave ripples (Diekelmann and Born, 2010), as well as the occurrence of BOLD fMRI hippocampal activity occurring during fast sleep spindles (Schabus et al., 2007). These hippocampus ROIs were created for the bilateral anterior and posterior hippocampus proper using the standard AAL atlas segmentations, separated into anterior and posterior sections along the longitudinal axes at the center-of-mass (Wendelken and Bunge, 2010). These segmentations therefore allow a focus on the hippocampus proper (thus not including parahippocampal gyrus regions).

Results

Gray matter volume associations with sleep spindle frequency

Contrary to our first prediction, no voxels in the thalamus demonstrated a significant relationship between gray matter volume and sleep spindle frequency, in either the slower (negative correlation) or faster (positive correlation) direction (all voxels $p > 0.001$; all cluster FWE corrected, $p > 0.2$).

Gray matter volume in exteroceptive and interoceptive sensory cortical ROIs did, however, significantly and negatively correlate with sleep spindle frequency. Specifically, greater gray matter volume in both bilateral auditory cortices (Heschl's gyrus; Fig. 1), as well as anterior and posterior regions of bilateral insula cortex were predictive of slower sleep spindle frequencies (Fig. 1 and Table 1A). Interestingly, and further compatible with a sleep protection hypothesis (Dang-Vu et al.,

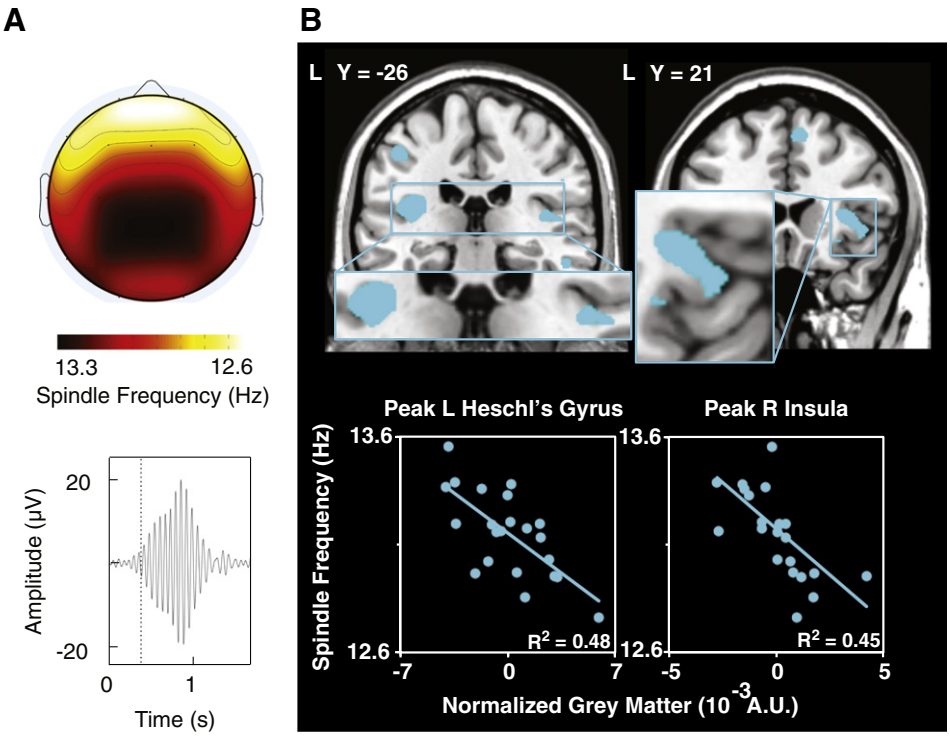

Fig. 1. Gray matter volume (GM) associations with slower sleep spindles within a priori regions of interest. A: (*left*) topographic plot of frontal dominant slower spindle frequency, with representative sleep spindle at electrode derivation Cz. B: (*right*) associations between slower sleep spindle frequencies and GM in bilateral auditory cortex (Heschl's gyrus) and in the left and right anterior and posterior insula, respectively, followed by scatterplots relating gray matter and spindle frequency at the peak voxels of the left Heschl's gyrus and right anterior cingulate clusters, respectively. Left image at MNI [*x y z*]: [−39 −26 14], right image at MNI: [38 21 2]. Statistical maps are displayed at $p < 0.005$.

2010a; De Gennaro and Ferrara, 2003; Landis et al., 2004), this same sleep spindle metric explained inter-individual differences in both sleep efficiency ($R^2 = 0.22$, $p = 0.027$; those with slower frequency spindles experienced fewer awakenings during the night), and less time spent awake after sleep onset (WASO; a metric of sleep stability), albeit non-significantly ($R^2 = 0.21$, $p = 0.06$). Beyond our a priori regions, uncorrected whole brain ($p < 0.001$ at the voxel level) analyses further revealed gray matter associations with slower frequency spindle activity in select frontal and temporal cortex regions (Supplemental results, Table S2).

Conversely, positive and significant bilateral associations were identified with gray matter volume in the hippocampus and sleep spindle frequency, specifically within posterior regions of the hippocampal complex (Fig. 2; Table 1B). This association was exclusive to the hippocampus, with no other regions approaching significance, even at the more liberal statistical threshold of the whole-brain analyses ($p < 0.001$ at the voxel level).

To further examine the robustness of these sleep spindle associations, SVC results were further submitted to a secondary level of family wise error correction across all ROIs combined (rather than considering each as independent). For the negative correlates of sleep spindle frequency (family of tests: thalamus, insula, auditory cortex), results in the insula as well as the auditory cortex remained significant at the cluster and peak-voxel level. Likewise, for positive correlates of sleep spindle frequency (family of tests: hippocampus, thalamus), results in the hippocampus remain significant at both levels of analysis.

Table 1
Gray matter volume correlates of sleep spindle frequency and slow waves (a priori regions).

Anatomical cluster		Local maxima (MNI)			Peak *Z*	$P_{SVC\text{-}cluster}$ non-stationary	$P_{SVC\text{-}peak\ (FWE)}$
Hemi	Label	*X*	*Y*	*Z*			
A. Gray matter volume negatively correlating with sleep spindle frequency							
L	Posterior insula	−40	−26	15	4.33	0.011	0.014
		−36	−8	20	3.81	0.029	0.037
L	Heschl's transverse gyrus	−39	−26	14	3.58	0.008	0.005
R		52	−19	8	3.72	0.020	0.016
		54	−15	7	3.56	0.022	0.022
L	Anterior insula	−35	−2	18	3.48	0.021	0.019
		−46	−5	14	3.62	0.050	0.047
		38	21	2	3.43	0.033	0.021
B. Gray matter volume positively correlating sleep spindle frequency							
L	Posterior hippocampus	−25	−27	−8	3.52	0.015	0.009
R		26	−31	−9	3.64	0.016	0.006
C. Gray *matter volume positively correlating with slow wave density*							
L	Basal forebrain/ hypothalamus	−2	2	−8	3.46	0.008	0.008
R		8	3	−5	3.16		0.018
D. Gray *matter volume positively correlating with slow wave amplitude*							
R	Orbital frontal cortex	2	34	−27	4.53	0.020	0.001
L		−1	34	−27	3.87	0.018	0.008
R	Cingulate cortex	7	−9	32	3.62	0.035	0.036
		8	−17	33	3.33		0.078

Sleep spindle frequency by topographic location

The choice to use a spindle measure averaged across three midline topographical locations (FZ, CZ, and PZ) was intended to incorporate both frontal-dominant slow frequency and parietal-dominant fast frequency spindles (De Gennaro and Ferrara, 2003). While this approach allows for a broad classification of individual-wise spindle frequency across topography, it may preclude sensitivity to any one of these

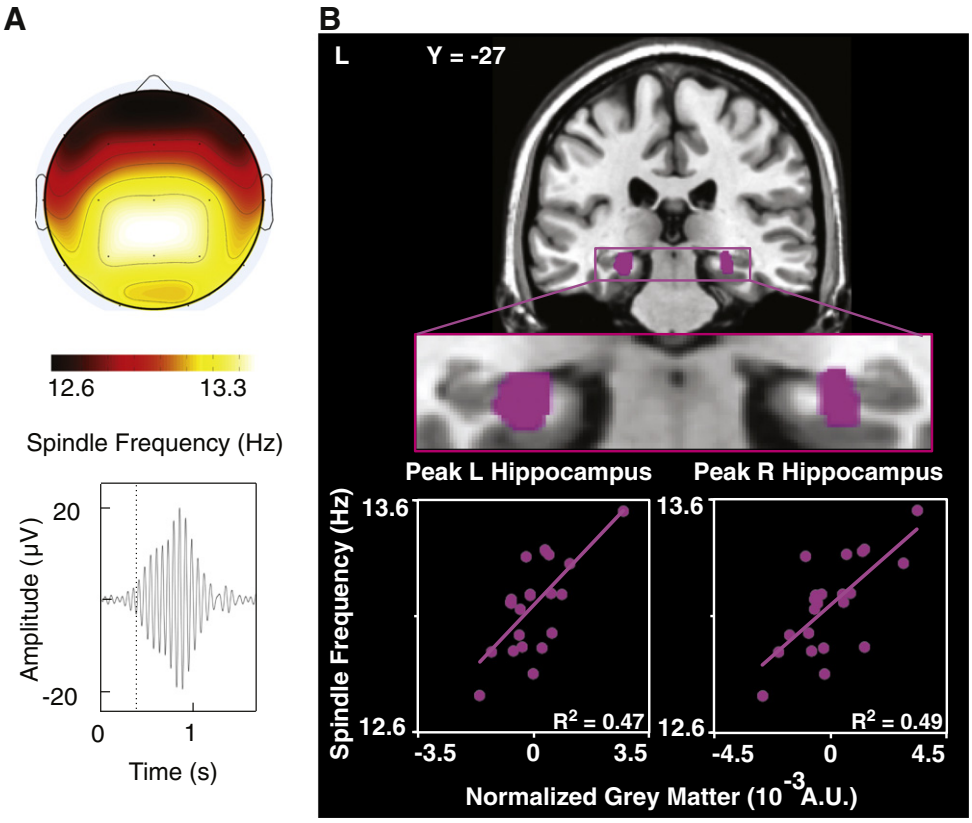

Fig. 2. Gray matter volume (GM) associations with faster sleep spindles within a priori regions of interest. A: (*left*) topographic plot of posterior dominant faster sleep spindle frequency. B: (*right*) positive association between faster sleep spindle frequencies and GM in bilateral posterior hippocampus, followed by scatterplots relating gray matter and spindle frequency at the peak voxels of the left and right hippocampus clusters, respectively. Image at MNI [*x y z*]: [−25 −27 −8]. Statistical maps are displayed at $p < 0.005$.

channels individually. It may also inadvertently bias results to the slow-dominant frequencies of FZ, or the fast-dominant frequencies of PZ, respectively. To explore these concerns, analyses were repeated using values derived from FZ, CZ, and PZ derivations separately, rather than using their integrated average. Results from each individual electrode (Supplemental Tables S5–S7 and Fig. S8) continue to support the current main findings. Specifically, significant spindle associations with gray matter volume in the hippocampus were identified for CZ and PZ derivations independently (not reaching significance for FZ). Further, significant associations with the sensory cortex were identified for FZ and CZ derivations independently (while not meeting significance for PZ). Together, the homology between these individual-electrode results and those in the above main results suggests that using a midline average approach provides a representative metric sensitive to spindles over both frontal slow frequency-dominant and parietal fast frequency-dominant topographic distributions.

Gray matter volume associations with slow waves

The density of NREM slow waves was positively correlated with gray matter volume in the basal forebrain — a region involved in the homeostatic regulation of sleep, including slow wave sleep (Kalinchuk et al., 2010; Modirrousta et al., 2007; Monti, 2011) (Esser et al., 2007) (Fig. 3; Table 1C). In contrast to density, the amplitude of slow waves was positively correlated with gray matter volume in medial prefrontal cortex, a region over which the greatest magnitude of slow wave are expressed, as is the great inter-individual difference in these waves (Carrier et al., 2011; Esser et al., 2007; Feinberg et al., 2011; Murphy et al., 2009; Vandewalle et al., 2009; Viola et al., 2007). Specifically, gray matter volume in both orbital frontal cortex as well as middle cingulate cortex was significantly and positively correlated with slow wave amplitude across individuals (Fig. 4; Table 1D). Counter to our predictions (Murphy et al., 2009), no voxels in the insula cortex demonstrated significant relationships with slow wave parameters at the whole-brain level (all voxels $p > 0.001$; all cluster FWE corrected, $p > 0.25$).

Beyond these ROIs, uncorrected whole-brain analyses ($p < 0.001$ at the voxel level) revealed that gray matter volume in the cerebellum, together with select regions in the parietal and temporal lobe also accounted for individual differences in slow wave density (Supplemental results, Table S3). Discrete frontal and temporal regions also positively correlated within slow wave amplitude, whereas gray matter in the occipital cortex and cerebellum negatively correlated with slow wave amplitude (Supplemental results, Table S4).

As with spindle analysis, to additionally determine the robustness of predictors of slow wave properties, SVC results were submitted to a secondary level of error correction across all ROIs combined, as described above (family of tests including: basal-forebrain/hypothalamus, insula, medial prefrontal cortex). Findings in the basal-forebrain/hypothalamus remain significant at both cluster and peak voxel levels, whereas results in the mesial orbital frontal cortex remain significant only at the peak voxel level. Results in the anterior cingulate cortex did not survive this secondary correction, emerging only at super-threshold levels of significance.

Finally, to examine the electrical source generation overlap with structural regions correlating with NREM slow waves, EEG current source density analysis was performed. EEG source localization of the slow waves, time-locked to the peak of the slow wave, revealed neural generators in remarkably similar medial frontal regions (Fig. 4); areas consistent with previous source analyses of slow waves (Murphy et al., 2009). Such homology between structural (gray matter volume) and functional (EEG source analysis) measures indicates that frontal brain morphology associated with slow wave expression converges

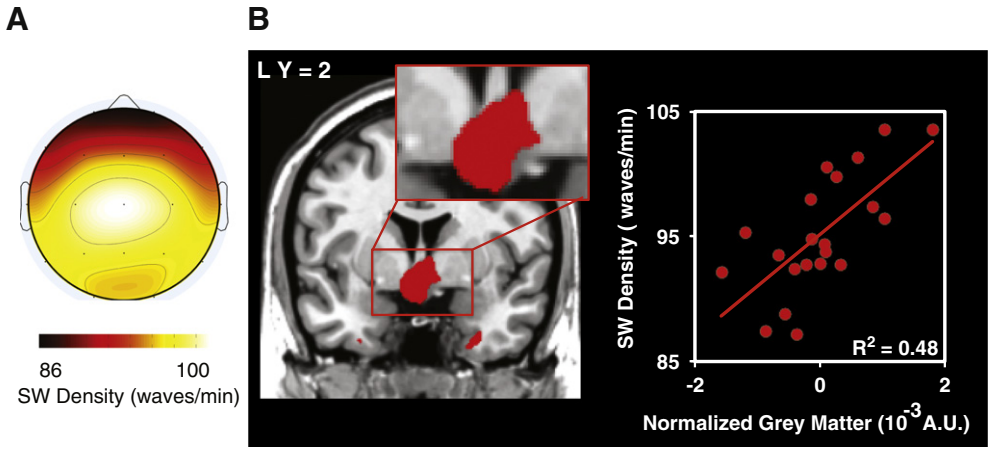

Fig. 3. Gray matter volume (GM) associations with NREM slow wave density within a priori regions of interest. A: (*left*) topographic plot of EEG slow wave (SW) density, demonstrating centro-parietal surface distribution, followed by B: (*middle*, *right*) positive association between SW density and GM in the basal forebrain/hypothalamus (coronal), followed by a scatterplot relating gray matter and SW density at the peak voxel of basal forebrain/hypothalamic cluster. Image at MNI [*x y z*]: [−2 2 −8]. Statistical maps are displayed at $p < 0.005$.

with overlapping frontal brain regions involved in the electrical generation of these slow waves.

Oscillation specificity effects

Two further analyses were conducted to determine the specificity of the sleep spindle and slow wave anatomical relationships. The first analysis aimed to determine whether the amount of time spent in NREM sleep, the brain state from which sleep spindles and slow waves arise, itself correlated with overlapping regional gray matter volume; a finding that would limit the specificity of any spindle and slow wave structural associations. No overlapping relationships were observed (Supplemental results, Fig. S6). Second, we examined whether oscillatory activity in a different frequency range (here, NREM alpha activity [8-11Hz) similarly correlated with the same gray matter regions as either spindles or slow waves; another finding that would challenge

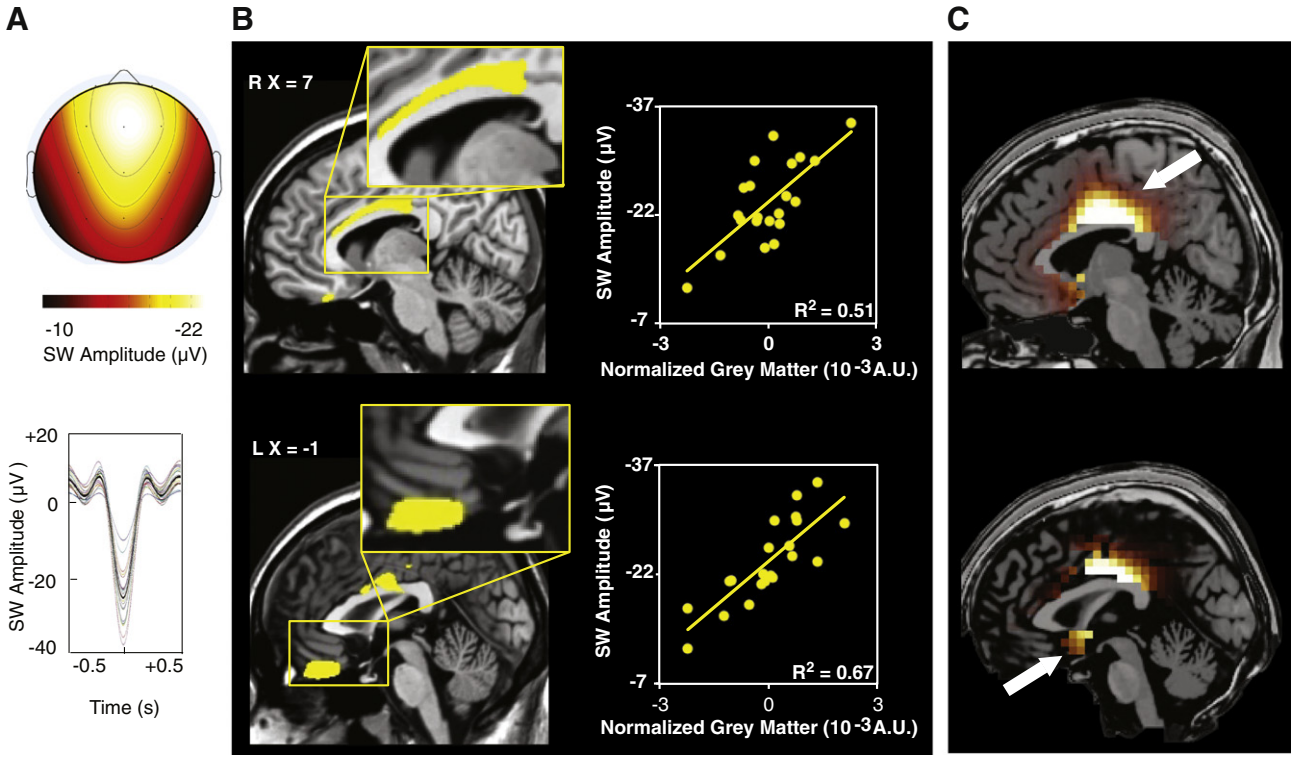

Fig. 4. Gray matter volume (GM) associations with NREM slow wave amplitude within a priori regions of interest. A: (*left*) topographic plot of EEG slow wave peak amplitude, demonstrating canonical frontal dominant surface distribution, with the corresponding average SW oscillation at electrode derivation Fz plotted for each subject (bold group average), B: (*middle*) positive association between SW amplitude and GM in middle cingulate and mesial orbital frontal cortex, each with strongly convergent anatomical findings (*right*) from sLORETA electrical source analyses of the peak SW amplitude, followed by scatterplot relating gray matter and SW amplitude at the peak voxels of the cingulate and orbital frontal clusters, respectively. Arrows designate similarity between GM correlates and source-generators of slow waves. Top image at MNI [*x y z*]: [7 −9 32], bottom image at MNI [*x y z*]: [−1 34 −27]. Statistical maps are displayed at $p < 0.005$.

the specificity of these associations. NREM alpha power was chosen since it represents a frequency band that is proximal to the spindle frequency range, and it is also known to be highly coherent across the scalp during slow wave sleep (Achermann and Borbély, 1998). Once again, no overlapping associations were identified (Supplemental results, Fig. S7).

Therefore, neither the total amount of time spent in NREM sleep, nor characteristics of other related NREM electrical oscillations, were associated with the anatomical brain regions correlating with with spindles and slow waves.

Discussion

Taken together, our findings demonstrate that inter-individual differences in gray matter volume account for variations in sleep EEG features, highlighting the notion that structural brain morphology is significantly associated with the qualitative and quantitative expression of human sleep physiology. In the following sections, we discuss functional implications and interpretations of these associations for each sleep oscillatory property separately.

Structural brain correlates of sleep spindle frequency

Consistent with theories of sleep protection against exogenous and endogenous conscious perception (De Gennaro and Ferrara, 2003), greater gray matter volume across individuals in both primary auditory and insular cortices was associated with progressively slower sleep spindle frequency. The associations in sensory areas may reflect the role of sleep spindles (of slower frequency) in the protection from sensory disruption (both extereoceptive and intereoceptive) during sleep. Indeed, focusing on audition as the prime exogenous route of sensory interference during sleep, recent findings have demonstrated that inter-individual variability in spindles over the sensory cortex predicts the extent to which sleep is preserved following experimental auditory stimulation (Dang-Vu et al., 2010a). Furthermore, circumstances of acquired hearing loss co-occur with reductions in both gray matter in auditory cortex and slow-frequency sleep spindles (Landgrebe et al., 2009; Scrofani et al., 1996).

Beyond exogenous (auditory) stimuli, endogenous sensory information, most notably pain, is similarly recognized to markedly disrupt sleep (Buenaver and Smith, 2007). Chronic pain has been associated independently with decreases in the number of sleep spindles (Landis et al., 2004) and reductions in insula cortex integrity (Kim et al., 2008). The spindle-insula cortex associations identified in the current study provide a basis on which these previously independent findings can be unite: the loss of insula gray matter in chronic pain may represent one putative mechanism that leads to decreases in slow sleep spindle activity, and with it, the susceptibility to interoceptive pain sensation during sleep. While this model remains speculative, future patient–cohort studies employing structural MRI, in conjunction with quantitative sensory testing and sleep EEG recordings will be able to elucidate such a mechanism.

In contrast to slower spindles, faster frequency sleep spindles (commonly in the range of 13–15 Hz) continue to be implicated in hippocampal-dependent memory processing (Diekelmann and Born, 2010). For example, inter-individual differences in sleep spindles, including fast sleep spindles, are associated with the benefit of sleep before learning, leading to enhanced hippocampal encoding ability (Mander et al., 2011), and sleep after learning in the offline consolidation of episodic memory (Gais et al., 2002; Rauchs et al., 2008; Saletin et al., 2011; Schabus et al., 2004, 2006, 2008). Likewise functional activity in the hippocampus coinciding with sleep spindles has been related to learning and memory processes (Andrade et al., 2011; Bergmann et al., 2012). Adding to this evidence, here we establish that the gray matter volume within the hippocampus predicts increasingly fast frequency spindles across individuals. While no memory tasks were included in the present study, this identified relationship is consistent with a broad collection of pathological circumstances describing not only marked impairments in sleep spindle activity, but co-occurring deficits in hippocampal gray matter and episodic memory, including Alzheimer's disease, Schizophrenia as well as sleep apnea (Barnes et al., 2009; Ferrarelli et al., 2007; Hedden and Gabrieli, 2004; Himanen et al., 2003; Joo et al., 2010; Kloepfer et al., 2009; Rauchs et al., 2008; Tamminga et al., 2010). Our findings suggest such features may be interrelated, offering a testable link between deficits in hippocampal structure, impoverished sleep spindle activity, and memory impairment.

Counter to our hypothesis, no structural relationships were identified between spindle frequency and the thalamus. One potential explanation for this lack of association is that the thalamus is not well segmented by T1-weighted structural MRI (Eggert et al., 2012). Irrespective, the absence of an association in the present data does not challenge the established role of the thalamus in generating spindles (Steriade et al., 1985). Instead, our results may be interpreted in the context of quantity relative to quality. While thalamic processes are critical for the instigation of sleep spindle events (quantity) (Roth et al., 2000; Steriade et al., 1985), the EEG expression of qualitative features of spindles (e.g. individual frequency) may be less dependent on thalamic structure and more dependent on down-stream cortical regions. This interpretation is consistent with previous EEG source analyses of sleep spindle demonstrating differential cortical (rather than thalamic) source associations of fast and slow sleep spindles (Anderer et al., 2001; Ventouras et al., 2007).

Beyond our a priori regions of interest, several additional regions were negatively correlated with spindle frequency at the whole-brain level. These included select frontal lobe regions, most prominent in dorsolateral prefrontal cortex. This is of note given the known frontal-dominant EEG surface expression of slow sleep spindles (De Gennaro and Ferrara, 2003; Schabus et al., 2007), and a recent report of congruent lateral prefrontal cortex fMRI activity associated with sleep spindle occurrence (Schabus et al., 2007). While gray matter associations with primary sensory and perceptual areas are consistent with a potential protective function of spindles, a role for human dorsolateral prefrontal cortex in sensory gating has recently been advanced (Mayer et al., 2009). Our findings offer tentative support to a framework where primary sensory and perceptual areas (here, auditory and insula cortices), in cooperation with high-order rating networks in dorsolateral prefrontal cortex, may form a sleep spindle regulating network capable of gating sensory interference and hence maintain the sleep state.

It should be noted that our regression technique relies on examining negative and positive contrasts of the same model to identify areas of gray matter volume predictive of inter-individual differences in slower and faster sleep spindle frequencies. As a result, each voxel can only be associated in a negative or a positive manner, and not predictive in both directions (although this does not preclude the possibility of generators common to fast and slow spindles).

Structural brain correlates of slow waves

The basal forebrain forms a major part of the neural circuitry that supports homeostatic sleep–wake regulation (Kalinchuk et al., 2010; Modirrousta et al., 2007; Monti, 2011). This homeostatic process is manifest in the cortical EEG by the slow wave (Esser et al., 2007), which responds in a proportional manner to sleep need (Dijk et al., 1993; Esser et al., 2007). While varying considerably between individuals, levels of slow wave expression under rested conditions are highly consistent within individuals in a trait-like manner (Tucker et al., 2007), potentially influenced by genotypic variations (Viola et al., 2007). Our findings indicate that brain structure affords one explanatory factor of inter-individual variance in slow waves, which itself may be determined by genotypic influence. Specifically, gray matter volume in the basal forebrain accounted for nearly 50% of the inter-individual variability in slow wave density; a finding anatomically consistent with the marked disruption of slow waves and their regulation that occurs

following lesions of the basal forebrain (Lai et al., 1999; Srividya et al., 2004). One testable prediction emerging from these findings is that gray matter integrity of the basal forebrain should serve as a predictor of inter-individual variability in homeostatic sleep regulation, indexed by slow waves, and perhaps most powerfully in response to the condition of sleep deprivation (Dijk et al., 1993).

Beyond density, slow waves have a known frontal-dominant topography of amplitude (Kurth et al., 2010; Riedner et al., 2007). Consistent with this topography, we show that gray matter volume within select midline prefrontal regions of the anterior cingulate and orbital frontal cortex positively predict slow wave amplitude. Offering convergent evidence, homologous medial prefrontal regions (peak source activity in the cingulate cortex) were identified using EEG source analysis of these slow waves; similar to previous EEG source analysis of slow waves (Murphy et al., 2009). While remaining speculative, such convergence across methods increasingly supports the midline frontal cortex as critical in the determination of NREM slow wave EEG generation. More broadly, the association between slow waves and regions of medial frontal cortex is consistent with ontogenetic differences in slow wave activity across the lifespan, with frontal cortex and slow waves expressing remarkably congruent developmental alterations early in life (Kurth et al., 2010) and pernicious reductions later in life (Buchmann et al., 2011b; Carrier et al., 2011).

While the insula cortex was a target region potentially accounting for inter-individual difference in slow waves, based on previous EEG source analysis (Murphy et al., 2009), no structural associations were identified, for either metric of NREM slow waves. While the insula cortex may be involved in the generation of slow waves (Murphy et al., 2009), gray matter volume does not appear to appear to be a strong determinant of the expression of these waves across individuals.

For slow wave density, two additional regions of association were observed in the whole brain analyses. First, gray matter volume in parahippocampal gyrus predicted individual differences in slow wave density, offering anatomical homology with regions expressing simultaneous activation during the coincidence of (rather than individual differences in) slow waves (Dang-Vu et al., 2008b). Second, gray matter volume in a number of sub-areas within the cerebellum further demonstrated a positive relationship with slow wave density. While unexpected, considering slow waves are known to derive from cortical sources, it is of note that similar cerebellar slow wave associations have been identified in fMRI studies (Dang-Vu et al., 2008b).

Our current analyses do not dissociate NREM K-complexes from slow waves, which themselves may have potentially influenced these slow wave findings. Despite their similarity in frequency and amplitude to slow waves (Amzica and Steriade, 1997), K-complexes make up a comparatively small proportion of the NREM EEG. As such, the influence of such K-complexes on current findings is likely modest.

Building on these results, prospective longitudinal studies will be required to determine the directional nature of these relationships, offering a complement to developmental cross-sectional approaches (Buchmann et al., 2011b), and examinations in clinical populations (Benson et al., 1996; Joo et al., 2010; Macey et al., 2002; O'Donoghue et al., 2005; van Kammen et al., 1988; Wiegand et al., 1991). Future structural investigations will likely benefit from examining additional anatomical metrics, including quantification of white matter fiber tracts between regions that may govern the propagation of electrical sleep oscillatory activity (Buchmann et al., 2011a; Piantoni et al., 2013). Together, such approaches will help define how the macroscopic structure of the human brain accounts of physiological sleep generation and expression, both in healthy populations as well as clinical disorders expressing co-morbid sleep abnormalities.

Acknowledgments

The authors would like to acknowledge Dr. Edwin Robertson for his helpful input on this manuscript. The authors would also like to thank Drs. Giulio Tononi, Reto Huber, and colleagues for their generous sharing of analytical software, and Stephanie Greer for technical assistance. Finally, the authors thank all the participants who took part in this study and the undergraduate research assistants who helped run the study. This research was supported by the National Institutes of Health: the National Institute on Aging (RO1AG031164 [MPW]) and the National Institute of Mental Health (R01MH093537 [MPW]), and the National Science Foundation (GRFP [JMS]).

Conflict of interest

The authors have no conflicts of interest to disclose regarding this work.

Appendix A. Supplementary data

Supplementary data to this article can be found online at http://dx.doi.org/10.1016/j.neuroimage.2013.06.021.

References

Achermann, P., Borbély, A.A., 1998. Coherence analysis of the human sleep electroencephalogram. Neuroscience 85, 1195–1208.
Achermann, P., Borbély, A.A., 2003. Mathematical models of sleep regulation. Front. Biosci. 8, s683–s693.
Aeschbach, D., Borbély, A., 1993. All-night dynamics of the human sleep EEG. J. Sleep Res. 2, 70–81.
Altena, E., Vrenken, H., Van Der Werf, Y.D., van den Heuvel, O.A., Van Someren, E.J.W., 2010. Reduced orbitofrontal and parietal gray matter in chronic insomnia: a voxel-based morphometric study. Biol. Psychiatry 67, 182–185.
Amzica, F., Steriade, M., 1997. The K-complex: its slow (<1-Hz) rhythmicity and relation to delta waves. Neurology 49, 952–959.
Anderer, P., Klösch, G., Gruber, G., Trenker, E., Pascual-Marqui, R.D., Zeitlhofer, J., Barbanoj, M.J., Rappelsberger, P., Saletu, B., 2001. Low-resolution brain electromagnetic tomography revealed simultaneously active frontal and parietal sleep spindle sources in the human cortex. Neuroscience 103, 581–592.
Andrade, K.C., Spoormaker, V.I., Dresler, M., Wehrle, R., Holsboer, F., Samann, P.G., Czisch, M., 2011. Sleep spindles and hippocampal functional connectivity in human NREM sleep. J. Neurosci. 31, 10331–10339.
Ansell, E.B., Rando, K., Tuit, K., Guarnaccia, J., Sinha, R., 2012. Cumulative adversity and smaller gray matter volume in medial prefrontal, anterior cingulate, and insula regions. Biol. Psychiatry 72, 57–64.
Ashburner, J., 2007. A fast diffeomorphic image registration algorithm. NeuroImage 38, 95–113.
Ashburner, J., Friston, K.J., 2000. Voxel-based morphometry—the methods. NeuroImage 11, 805–821.
Barnes, J., Bartlett, J.W., van de Pol, L.A., Loy, C.T., Scahill, R.I., Frost, C., Thompson, P., Fox, N.C., 2009. A meta-analysis of hippocampal atrophy rates in Alzheimer's disease. Neurobiol. Aging 30, 1711–1723.
Bela, C., Monika, B., Marton, T., Istvan, K., 2007. Valproate selectively reduces EEG activity in anterior parts of the cortex in patients with idiopathic generalized epilepsy. A low resolution electromagnetic tomography (LORETA) study. Epilepsy Res. 75, 186–191.
Bendlin, B.B., Ries, M.L., Lazar, M., Alexander, A.L., Dempsey, R.J., Rowley, H.A., Sherman, J.E., Johnson, S.C., 2008. Longitudinal changes in patients with traumatic brain injury assessed with diffusion-tensor and volumetric imaging. NeuroImage 42, 503–514.
Benedetti, F., Radaelli, D., Poletti, S., Falini, A., Cavallaro, R., Dallaspezia, S., Riccaboni, R., Scotti, G., Smeraldi, E., 2011. Emotional reactivity in chronic schizophrenia: structural and functional brain correlates and the influence of adverse childhood experiences. Psychol. Med. 41, 509–519.
Benedetti, F., Poletti, S., Radaelli, D., Pozzi, E., Giacosa, C., Ruffini, C., Falini, A., Smeraldi, E., 2012. Caudate gray matter volume in obsessive-compulsive disorder is influenced by adverse childhood experiences and ongoing drug treatment. J. Clin. Psychopharmacol. 32, 544–547.
Benson, K.L., Sullivan, E.V., Lim, K.O., Lauriello, J., Zarcone Jr., V.P., Pfefferbaum, A., 1996. Slow wave sleep and computed tomographic measures of brain morphology in schizophrenia. Psychiatry Res. 60, 125–134.
Bergmann, T.O., Molle, M., Diedrichs, J., Born, J., Siebner, H.R., 2012. Sleep spindle-related reactivation of category-specific cortical regions after learning face-scene associations. NeuroImage 59, 2733–2742.
Buchmann, A., Kurth, S., Ringli, M., Geiger, A., Jenni, O.G., Huber, R., 2011a. Anatomical markers of sleep slow wave activity derived from structural magnetic resonance images. J. Sleep Res. 20, 506–513.
Buchmann, A., Ringli, M., Kurth, S., Schaerer, M., Geiger, A., Jenni, O.G., Huber, R., 2011b. EEG sleep slow–wave activity as a mirror of cortical maturation. Cereb. Cortex 21, 607–615.
Buenaver, L.F., Smith, M.T., 2007. Sleep in rheumatic diseases and other painful conditions. Curr. Treat. Options Neurol. 9, 325–336.
Carrier, J., Viens, I., Poirier, G., Robillard, R., Lafortune, M., Vandewalle, G., Martin, N., Barakat, M., Paquet, J., Filipini, D., 2011. Sleep slow wave changes during the middle years of life. Eur. J. Neurosci. 33, 758–766.

Celle, S., Roche, F., Peyron, R., Faillenot, I., Laurent, B., Pichot, V., Barthélémy, J.-C., Sforza, E., 2010. Lack of specific gray matter alterations in restless legs syndrome in elderly subjects. J. Neurol. 257, 344–348.

Clemens, B., Bank, J., Piros, P., Bessenyei, M., Veto, S., Toth, M., Kondakor, I., 2008. Three-dimensional localization of abnormal EEG activity in migraine: a low resolution electromagnetic tomography (LORETA) study of migraine patients in the pain-free interval. Brain Topogr. 21, 36–42.

Clemens, B., Piros, P., Bessenyei, M., Varga, E., Puskas, S., Fekete, I., 2009. The electrophysiological "delayed effect" of focal interictal epileptiform discharges. A low resolution electromagnetic tomography (LORETA) study. Epilepsy Res. 85, 270–278.

Contreras, D., Steriade, M., 1996. Spindle oscillation in cats: the role of corticothalamic feedback in a thalamically generated rhythm. J. Physiol. (Lond) 490 (Pt 1), 159–179.

D'Agata, F., Caroppo, P., Boghi, A., Coriasco, M., Caglio, M., Baudino, B., Sacco, K., Cauda, F., Geda, E., Bergui, M., Geminiani, G., Bradac, G.B., Orsi, L., Mortara, P., 2011. Linking coordinative and executive dysfunctions to atrophy in spinocerebellar ataxia 2 patients. Brain Struct. Funct. 216, 275–288.

Dang-Vu, T., Schabus, M., Boly, M., Bonjean, M., Darsaud, A., Degueldre, C., Phillips, C., Maquet, P., 2008a. Processing of sounds during sleep spindles in humans: an EEG/fMRI study of auditory stimulation in NREM sleep. Sleep 31, A4.

Dang-Vu, T.T., Schabus, M., Desseilles, M., Albouy, G., Boly, M., Darsaud, A., Gais, S., Rauchs, G., Sterpenich, V., Vandewalle, G., Carrier, J., Moonen, G., Balteau, E., Degueldre, C., Luxen, A., Phillips, C., Maquet, P., 2008b. Spontaneous neural activity during human slow wave sleep. Proc. Natl. Acad. Sci. U.S.A. 105, 15160–15165.

Dang-Vu, T.T., McKinney, S.M., Buxton, O.M., Solet, J.M., Ellenbogen, J.M., 2010a. Spontaneous brain rhythms predict sleep stability in the face of noise. Curr. Biol. 20, R626–R627.

Dang-Vu, T.T., Schabus, M., Desseilles, M., Sterpenich, V., Bonjean, M., Maquet, P., 2010b. Functional neuroimaging insights into the physiology of human sleep. Sleep 33, 1589–1603.

De Gennaro, L., Ferrara, M., 2003. Sleep spindles: an overview. Sleep Med. Rev. 7, 423–440.

De Gennaro, L., Ferrara, M., Vecchio, F., Curcio, G., Bertini, M., 2005. An electroencephalographic fingerprint of human sleep. NeuroImage 26, 114–122.

Diekelmann, S., Born, J., 2010. The memory function of sleep. Nat. Rev. Neurosci. 11, 114–126.

Dijk, D.J., Hayes, B., Czeisler, C.A., 1993. Dynamics of electroencephalographic sleep spindles and slow wave activity in men: effect of sleep deprivation. Brain Res. 626, 190–199.

Dumontheil, I., Houlton, R., Christoff, K., Blakemore, S.-J., 2010. Development of relational reasoning during adolescence. Dev. Sci. 13, F15–F24.

Eckert, M.A., Lombardino, L.J., Walczak, A.R., Bonihla, L., Leonard, C.M., Binder, J.R., 2008. Manual and automated measures of superior temporal gyrus asymmetry: concordant structural predictors of verbal ability in children. NeuroImage 41, 813–822.

Eggert, L.D., Sommer, J., Jansen, A., Kircher, T., Konrad, C., 2012. Accuracy and reliability of automated gray matter segmentation pathways on real and simulated structural magnetic resonance images of the human brain. PloS one 7, e45081.

Esser, S.K., Hill, S.L., Tononi, G., 2007. Sleep homeostasis and cortical synchronization: I Modeling the effects of synaptic strength on sleep slow waves. Sleep 30, 1617–1630.

Feinberg, I., de Bie, E., Davis, N.M., Campbell, I.G., 2011. Topographic differences in the adolescent maturation of the slow wave EEG during NREM sleep. Sleep 34, 325–333.

Ferrarelli, F., Huber, R., Peterson, M.J., Massimini, M., Murphy, M., Riedner, B.A., Watson, A., Bria, P., Tononi, G., 2007. Reduced sleep spindle activity in schizophrenia patients. Am. J. Psychiatry 164, 483–492.

Fischl, B., Dale, A.M., 2000. Measuring the thickness of the human cerebral cortex from magnetic resonance images. Proc. Natl. Acad. Sci. U. S. A. 97, 11050–11055.

Gais, S., Molle, M., Helms, K., Born, J., 2002. Learning-dependent increases in sleep spindle density. J. Neurosci. 22, 6830–6834.

Giorgio, A., Watkins, K.E., Chadwick, M., James, S., Winmill, L., Douaud, G., De Stefano, N., Matthews, P.M., Smith, S.M., Johansen-Berg, H., James, A.C., 2010. Longitudinal changes in grey and white matter during adolescence. NeuroImage 49, 94–103.

Goel, N., Banks, S., Mignot, E., Dinges, D.F., 2009. PER3 polymorphism predicts cumulative sleep homeostatic but not neurobehavioral changes to chronic partial sleep deprivation. PLoS One 4, e5874.

Gong, Q.-Y., Sluming, V., Mayes, A., Keller, S., Barrick, T., Cezayirli, E., Roberts, N., 2005. Voxel-based morphometry and stereology provide convergent evidence of the importance of medial prefrontal cortex for fluid intelligence in healthy adults. NeuroImage 25, 1175–1186.

Hagemann, D., Hewig, J., Walter, C., Naumann, E., 2008. Skull thickness and magnitude of EEG alpha activity. Clin. Neurophysio. 119, 1271–1280.

Hedden, T., Gabrieli, J.D.E., 2004. Insights into the ageing mind: a view from cognitive neuroscience. Nat. Rev. Neurosci. 5, 87–96.

Himanen, S.-L., Virkkala, J., Huupponen, E., Hasan, J., 2003. Spindle frequency remains slow in sleep apnea patients throughout the night. Sleep Med. 4, 229–234.

Huber, R., Ghilardi, M.F., Massimini, M., Tononi, G., 2004. Local sleep and learning. Nature 430, 78–81.

Isotani, T., Lehmann, D., Pascual-Marqui, R.D., Kochi, K., Wackermann, J., Saito, N., Yagyu, T., Kinoshita, T., Sasada, K., 2001. EEG source localization and global dimensional complexity in high- and low- hypnotizable subjects: a pilot study. Neuropsychobiology 44, 192–198.

Jasper, H.H., 1958. The ten-twenty electrode system of the International Federation. Electroen. Clin. Neuro. 10, 367–380.

Joo, E.Y., Tae, W.S., Kim, S.T., Hong, S.B., 2009. Gray matter concentration abnormality in brains of narcolepsy patients. Korean J. Radiol. 10, 552–558.

Joo, E.Y., Tae, W.S., Lee, M.J., Kang, J.W., Park, H.S., Lee, J.Y., Suh, M., Hong, S.B., 2010. Reduced brain gray matter concentration in patients with obstructive sleep apnea syndrome. Sleep 33, 235–241.

Kalinchuk, A.V., McCarley, R.W., Porkka-Heiskanen, T., Basheer, R., 2010. Sleep deprivation triggers inducible nitric oxide-dependent nitric oxide production in wake-active basal forebrain neurons. J. Neurosci. 30, 13254–13264.

Kanai, R., Rees, G., 2011. The structural basis of inter-individual differences in human behaviour and cognition. Nat. Rev. Neurosci. 12, 231–242.

Kim, J.H., Suh, S.-I., Seol, H.Y., Oh, K., Seo, W.-K., Yu, S.-W., Park, K.-W., Koh, S.-B., 2008. Regional grey matter changes in patients with migraine: a voxel-based morphometry study. Cephalalgia 28, 598–604.

Kloepfer, C., Riemann, D., Nofzinger, E.A., Feige, B., Unterrainer, J., O'Hara, R., Sorichter, S., Nissen, C., 2009. Memory before and after sleep in patients with moderate obstructive sleep apnea. J. Clin. Sleep Med. 5, 540–548.

Koutsouleris, N., Schmitt, G.J.E., Gaser, C., Bottlender, R., Scheuerecker, J., McGuire, P., Burgermeister, B., Born, C., Reiser, M., Möller, H.-J., Meisenzahl, E.M., 2009. Neuroanatomical correlates of different vulnerability states for psychosis and their clinical outcomes. Br. J. Psychiatry 195, 218–226.

Kurth, S., Jenni, O.G., Riedner, B.A., Tononi, G., Carskadon, M.A., Huber, R., 2010. Characteristics of sleep slow waves in children and adolescents. Sleep 33, 475–480.

Laarne, P.H., Tenhunen-Eskelinen, M.L., Hyttinen, J.K., Eskola, H.J., 2000. Effect of EEG electrode density on dipole localization accuracy using two realistically shaped skull resistivity models. Brain Topogr. 12, 249–254.

Lai, Y.Y., Shalita, T., Hajnik, T., Wu, J.P., Kuo, J.S., Chia, L.G., Siegel, J.M., 1999. Neurotoxic N-methyl-D-aspartate lesion of the ventral midbrain and mesopontine junction alters sleep-wake organization. Neuroscience 90, 469–483.

Landgrebe, M., Langguth, B., Rosengarth, K., Braun, S., Koch, A., Kleinjung, T., May, A., de Ridder, D., Hajak, G., 2009. Structural brain changes in tinnitus: grey matter decrease in auditory and non-auditory brain areas. NeuroImage 46, 213–218.

Landis, C.A., Lentz, M.J., Rothermel, J., Buchwald, D., Shaver, J.L.F., 2004. Decreased sleep spindles and spindle activity in midlife women with fibromyalgia and pain. Sleep 27, 741–750.

Macey, P.M., Henderson, L.A., Macey, K.E., Alger, J.R., Frysinger, R.C., Woo, M.A., Harper, R.K., Yan-Go, F.L., Harper, R.M., 2002. Brain morphology associated with obstructive sleep apnea. Am. J. Respir. Crit. Care Med. 166, 1382–1387.

Mak, H.K.-F., Zhang, Z., Yau, K.K.-W., Zhang, L., Chan, Q., Chu, L.-W., 2011. Efficacy of voxel-based morphometry with DARTEL and standard registration as imaging biomarkers in Alzheimer's disease patients and cognitively normal older adults at 3.0 Tesla MR imaging. J. Alzheimers Dis. 23 (4), 655–664.

Maldjian, J.A., Laurienti, P.J., Kraft, R.A., Burdette, J.H., 2003. An automated method for neuroanatomic and cytoarchitectonic atlas-based interrogation of fMRI data sets. NeuroImage 19, 1233–1239.

Mander, B.A., Santhanam, S., Saletin, J.M., Walker, M.P., 2011. Wake deterioration and sleep restoration of human learning. Curr. Biol. 21, R183–R184.

Maquet, P., Degueldre, C., Delfiore, G., Aerts, J., Péters, J.M., Luxen, A., Franck, G., 1997. Functional neuroanatomy of human slow wave sleep. J. Neurosci. 17, 2807–2812.

Massimini, M., Ferrarelli, F., Esser, S.K., Riedner, B.A., Huber, R., Murphy, M., Peterson, M.J., Tononi, G., 2007. Triggering sleep slow waves by transcranial magnetic stimulation. Proc. Natl. Acad. Sci. U.S.A 104, 8496–8501.

Mayer, A.R., Hanlon, F.M., Franco, A.R., Teshiba, T.M., Thoma, R.J., Clark, V.P., Canive, J.M., 2009. The neural networks underlying auditory sensory gating. NeuroImage 44, 182–189.

Mazziotta, J., Toga, A., Evans, A., Fox, P., Lancaster, J., Zilles, K., Woods, R., Paus, T., Simpson, G., Pike, B., Holmes, C., Collins, L., Thompson, P., MacDonald, D., Iacoboni, M., Schormann, T., Amunts, K., Palomero-Gallagher, N., Geyer, S., Parsons, L., Narr, K., Kabani, N., Le Goualher, G., Feidler, J., Smith, K., Boomsma, D., Hulshoff Pol, H., Cannon, T., Kawashima, R., Mazoyer, B., 2001. A four-dimensional probabilistic atlas of the human brain. J. Am. Med. Inform. Assoc. 8, 401–430.

Mistlberger, R., Bergmann, B., Rechtschaffen, A., 1987. Period-amplitude analysis of rat electroencephalogram: effects of sleep deprivation and exercise. Sleep 10, 508–522.

Modirrousta, M., Mainville, L., Jones, B.E., 2007. Dynamic changes in GABAA receptors on basal forebrain cholinergic neurons following sleep deprivation and recovery. BMC Neurosci. 8, 15.

Mongrain, V., Carrier, J., Dumont, M., 2006. Difference in sleep regulation between morning and evening circadian types as indexed by antero-posterior analyses of the sleep EEG. Eur. J. Neurosci. 23, 497–504.

Monti, J.M., 2011. Serotonin control of sleep–wake behavior. Sleep Med. Rev. 15, 269–281.

Mueller, S.C., Merke, D.P., Leschek, E.W., Fromm, S., Vanryzin, C., Ernst, M., 2011. Increased medial temporal lobe and striatal grey-matter volume in a rare disorder of androgen excess: a voxel-based morphometry (VBM) study. Int. J. Neuropsychopharmacol. 14, 445–457.

Murphy, M., Riedner, B., Huber, R., Massimini, M., Ferrarelli, F., Tononi, G., 2009. Source modeling sleep slow waves. Proc. Natl. Acad. Sci. U. S. A. 106 (5), 1608–1613.

Neylan, T.C., Mueller, S.G., Wang, Z., Metzler, T.J., Lenoci, M., Truran, D., Marmar, C.R., Weiner, M.W., Schuff, N., 2010. Insomnia severity is associated with a decreased volume of the CA3/dentate gyrus hippocampal subfield. Biol. Psychiatry 68, 494–496.

Nichols, T., Hayasaka, S., 2003. Controlling the familywise error rate in functional neuroimaging: a comparative review. Stat. Methods Med. Res. 12, 419–446.

O'Donoghue, F.J., Briellmann, R.S., Rochford, P.D., Abbott, D.F., Pell, G.S., Chan, C.H.P., Tarquinio, N., Jackson, G.D., Pierce, R.J., 2005. Cerebral structural changes in severe obstructive sleep apnea. Am. J. Respir. Crit. Care Med. 171, 1185–1190.

Pascual-Marqui, R.D., 2002. Standardized low-resolution brain electromagnetic tomography (sLORETA): technical details. Methods Find. Exp. Clin. Pharmacol. 24 (Suppl. D), 5–12.

Pascual-Marqui, R.D., Lehmann, D., Koenig, T., Kochi, K., Merlo, M.C., Hell, D., Koukkou, M., 1999. Low resolution brain electromagnetic tomography (LORETA) functional imaging in acute, neuroleptic-naive, first-episode, productive schizophrenia. Psychiatry Res. 90, 169–179.

Pereira, J.M.S., Xiong, L., Acosta-Cabronero, J., Pengas, G., Williams, G.B., Nestor, P.J., 2010. Registration accuracy for VBM studies varies according to region and degenerative disease grouping. NeuroImage 49, 2205–2215.
Petrides, M., Pandya, D.N., 1999. Dorsolateral prefrontal cortex: comparative cytoarchitectonic analysis in the human and the macaque brain and corticocortical connection patterns. Eur. J. Neurosci. 11, 1011–1036.
Piantoni, G., Poil, S.S., Linkenkaer-Hansen, K., Verweij, I.M., Ramautar, J.R., Van Someren, E.J., Van Der Werf, Y.D., 2013. Individual differences in white matter diffusion affect sleep oscillations. J. Neurosci. 33, 227–233.
Pivik, R.T., Joncas, S., Busby, K.A., 1999. Sleep spindles and arousal: the effects of age and sensory stimulation. Sleep Res. Online 2, 89–100.
Ponomarev, V.A., Gurskaia, O.E., Kropotov Iu, D., Artiushkova, L.V., Muller, A., 2010. The comparison of clustering methods of EEG independent components in healthy subjects and patients with post concussion syndrome after traumatic brain injury. Fiziol. Cheloveka 36, 5–14.
Rauchs, G., Schabus, M., Parapatics, S., Bertran, F., Clochon, P., Hot, P., Denise, P., Desgranges, B., Eustache, F., Gruber, G., Anderer, P., 2008. Is there a link between sleep changes and memory in Alzheimer's disease? Neuroreport 19, 1159–1162.
Rechtschaffen, A., Kales, A., 1968. A Manual of Standardized Terminology, Techniques and Scoring System for Sleep Stages of Human Subjects. US Public Health Service, US Government Printing Office.
Ridgway, G.R., Omar, R., Ourselin, S., Hill, D.L.G., Warren, J.D., Fox, N.C., 2009. Issues with threshold masking in voxel-based morphometry of atrophied brains. NeuroImage 44, 99–111.
Riedner, B.A., Vyazovskiy, V.V., Huber, R., Massimini, M., Esser, S., Murphy, M., Tononi, G., 2007. Sleep homeostasis and cortical synchronization: III. A high-density EEG study of sleep slow waves in humans. Sleep 30, 1643–1657.
Roth, C., Jeanmonod, D., Magnin, M., Morel, A., Achermann, P., 2000. Effects of medial thalamotomy and pallido-thalamic tractotomy on sleep and waking EEG in pain and Parkinsonian patients. Clin. Neurophysiol. 111, 1266–1275.
Rusterholz, T., Achermann, P., 2011. Topographical aspects in the dynamics of sleep homeostasis in young men: individual patterns. BMC Neurosci. 12, 84.
Saletin, J.M., Goldstein, A.N., Walker, M.P., 2011. The role of sleep in directed forgetting and remembering of human memories. Cereb. Cortex. http://dx.doi.org/10.1093/cercor/bhr034.
Schabus, M., Gruber, G., Parapatics, S., Sauter, C., Klosch, G., Anderer, P., Klimesch, W., Saletu, B., Zeitlhofer, J., 2004. Sleep spindles and their significance for declarative memory consolidation. Sleep 27, 1479–1485.
Schabus, M., Hodlmoser, K., Gruber, G., Sauter, C., Anderer, P., Klosch, G., Parapatics, S., Saletu, B., Klimesch, W., Zeitlhofer, J., 2006. Sleep spindle-related activity in the human EEG and its relation to general cognitive and learning abilities. Eur. J. Neurosci. 23, 1738–1746.
Schabus, M., Dang-Vu, T.T., Albouy, G., Balteau, E., Boly, M., Carrier, J., Darsaud, A., Degueldre, C., Desseilles, M., Gais, S., Phillips, C., Rauchs, G., Schnakers, C., Sterpenich, V., Vandewalle, G., Luxen, A., Maquet, P., 2007. Hemodynamic cerebral correlates of sleep spindles during human non-rapid eye movement sleep. Proc. Natl. Acad. Sci. U. S. A. 104, 13164–13169.
Schabus, M., Hoedlmoser, K., Pecherstorfer, T., Anderer, P., Gruber, G., Parapatics, S., Sauter, C., Kloesch, G., Klimesch, W., Saletu, B., Zeitlhofer, J., 2008. Interindividual sleep spindle differences and their relation to learning-related enhancements. Brain Res. 1191, 127–135.
Schmitz, S.K., Hjorth, J.J.J., Joemai, R.M.S., Wijntjes, R., Eijgenraam, S., de Bruijn, P., Georgiou, C., de Jong, A.P.H., van Ooyen, A., Verhage, M., Cornelisse, L.N., Toonen, R.F., Veldkamp, W., 2011. Automated analysis of neuronal morphology, synapse number and synaptic recruitment. J. Neurosci. Methods 195, 185–193.
Scrofani, A., Cioni, M., Filetti, S., Lanaia, F., Pennisi, G., Bella, R., Grasso, A., 1996. Changes in sleep spindle activity of subject with chronic somatosensitive and sensorial deficits. Preliminary results. Ital. J. Neurol. Sci. 17, 423–428.
Srividya, R., Mallick, H.N., Kumar, V.M., 2004. Sleep changes produced by destruction of medial septal neurons in rats. Neuroreport 15, 1831–1835.
Steriade, M., Deschênes, M., Domich, L., Mulle, C., 1985. Abolition of spindle oscillations in thalamic neurons disconnected from nucleus reticularis thalami. J. Neurophysiol. 54, 1473–1497.
Steriade, M., McCormick, D.A., Sejnowski, T.J., 1993. Thalamocortical oscillations in the sleeping and aroused brain. Science 262, 679–685.
Szymusiak, R., 1995. Magnocellular nuclei of the basal forebrain: substrates of sleep and arousal regulation. Sleep 18, 478–500.
Tamminga, C.A., Stan, A.D., Wagner, A.D., 2010. The hippocampal formation in schizophrenia. Am. J. Psychiatry 167, 1178–1193.
Thompson, P.M., Cannon, T.D., Narr, K.L., van Erp, T., Poutanen, V.P., Huttunen, M., Lonnqvist, J., Standertskjold-Nordenstam, C.G., Kaprio, J., Khaledy, M., Dail, R., Zoumalan, C.I., Toga, A.W., 2001. Genetic influences on brain structure. Nat. Neurosci. 4, 1253–1258.
Tislerova, B., Brunovsky, M., Horacek, J., Novak, T., Kopecek, M., Mohr, P., Krajca, V., 2008. LORETA functional imaging in antipsychotic-naive and olanzapine-, clozapine- and risperidone-treated patients with schizophrenia. Neuropsychobiology 58, 1–10.
Tononi, G., Cirelli, C., 2006. Sleep function and synaptic homeostasis. Sleep Med. Rev. 10, 49–62.
Tucker, A.M., Dinges, D.F., Van Dongen, H.P., 2007. Trait interindividual differences in the sleep physiology of healthy young adults. J. Sleep Res. 16, 170–180.
van der Kooy, D., McGinty, J.F., Koda, L.Y., Gerfen, C.R., Bloom, F.E., 1982. Visceral cortex: a direct connection from prefrontal cortex to the solitary nucleus in rat. Neurosci. Lett. 33, 123–127.
van Kammen, D.P., van Kammen, W.B., Peters, J., Goetz, K., Neylan, T., 1988. Decreased slow-wave sleep and enlarged lateral ventricles in schizophrenia. Neuropsychopharmacology 1, 265–271.
Vandewalle, G., Archer, S.N., Wuillaume, C., Balteau, E., Degueldre, C., Luxen, A., Maquet, P., Dijk, D.-J., 2009. Functional magnetic resonance imaging-assessed brain responses during an executive task depend on interaction of sleep homeostasis, circadian phase, and PER3 genotype. J. Neurosci. 29, 7948–7956.
Veiga, H., Deslandes, A., Cagy, M., Fiszman, A., Piedade, R.A., Ribeiro, P., 2003. Neurocortical electrical activity tomography in chronic schizophrenics. Arq. Neuropsiquiatr. 61, 712–717.
Ventouras, E.M., Alevizos, I., Ktonas, P.Y., Tsekou, H., Paparrigopoulos, T., Kalatzis, I., Soldatos, C.R., Nikiforidis, G., 2007. Independent components of sleep spindles. Conf. Proc. IEEE Eng. Med. Biol. Soc. 2007, 4002–4005.
Viola, A.U., Archer, S.N., James, L.M., Groeger, J.A., Lo, J.C.Y., Skene, D.J., von Schantz, M., Dijk, D.-J., 2007. PER3 polymorphism predicts sleep structure and waking performance. Curr. Biol. 17, 613–618.
Viola, A.U., Chellappa, S.L., Archer, S.N., Pugin, F., Gotz, T., Dijk, D.J., Cajochen, C., 2012. Interindividual differences in circadian rhythmicity and sleep homeostasis in older people: effect of a PER3 polymorphism. Neurobiol. Aging 33 (1010), e1017–e1027.
Wendelken, C., Bunge, S.A., 2010. Transitive inference: distinct contributions of rostrolateral prefrontal cortex and the hippocampus. J. Cogn. Neurosci. 22, 837–847.
Werth, E., Achermann, P., Dijk, D.J., Borbély, A.A., 1997. Spindle frequency activity in the sleep EEG: individual differences and topographic distribution. Electroencephalogr. Clin. Neurophysiol. 103, 535–542.
Wiegand, M., Moller, A.A., Schreiber, W., Lauer, C., Krieg, J.C., 1991. Brain morphology and sleep EEG in patients with Huntington's disease. Eur. Arch. Psychiatry Clin. Neurosci. 240, 148–152.
Wolk, D.A., Price, J.C., Saxton, J.A., Snitz, B.E., James, J.A., Lopez, O.L., Aizenstein, H.J., Cohen, A.D., Weissfeld, L.A., Mathis, C.A., Klunk, W.E., De-Kosky, S.T., 2009. Amyloid imaging in mild cognitive impairment subtypes. Ann. Neurol. 65, 557–568.
Yaouhi, K., Bertran, F., Clochon, P., Mézenge, F., Denise, P., Foret, J., Eustache, F., Desgranges, B., 2009. A combined neuropsychological and brain imaging study of obstructive sleep apnea. J. Sleep Res. 18, 36–48.